Noise color shapes power grid stochastic responses

Longxin Yang and Xiaozhu Zhang (张潇竹)*

MOE Key Laboratory of Advanced Micro-Structured Materials, and School of Physical Science and Engineering, Tongji University, Shanghai, People's Republic of China

and National Key Laboratory of Autonomous Intelligent Unmanned Systems, MOE Frontiers Science Center for Intelligent Autonomous Systems, and Shanghai Research Institute of Intelligence Science and Technology, Tongji University, Shanghai, People's Republic of China

(Received 28 December 2025; revised 21 July 2026; accepted 14 October 2026; published 2 November 2026)

Real-world networked systems, such as power grids, operate inevitably under various types of noise originating from distinctive sources, which brings uncertainty and risks for systems' safe operation. As a major noise type, colored noise may enter the power system through multiple channels. For instance, through the large-scale integration of renewable energy sources and the demand-side power fluctuations, colored noise impinges on the stochastic frequency responses of power grids in a way that is not yet fully understood to date. In this work we systematically investigate the impact of noise color on the statistical properties of dynamic power grid frequency responses. Through abundant numerical simulations of a paradigmatic Kuramoto-like grid model subject to $1/f^b$ noise with a tunable color, we demonstrate that noise with a steeper power spectrum ($b \gtrsim 1$) dominated by low-frequency components drives power grid responses into a regime of nonstationarity and non-Gaussianity, while the responses are Gaussian for $b \lesssim 1$ despite the non-Gaussianity of the noise. We further show that this transition at $b \approx 1$ occurs independent of the specific topological structure underlying the power grid systems. This suggests that the intermittent renewable power feed-in with Kolmogorov exponent 5/3 may be a source of the observed non-Gaussian distribution of power grid frequency. Our results may thereby help better understand and control the collective frequency fluctuations in modern power grids.

DOI: 10.1103/tr4w-yrs1

I. INTRODUCTION

As the largest artificial infrastructure network supporting almost every facet of our daily life, power systems are operating under a wide range of noise with diverse origins and varied characteristics [1], just like any other real-world complex systems. Apart from the ubiquitous thermal white noise and the pink noise rising from electronic elements, the fluctuations in the power feed-in and in the power consumption pose a significant challenge in the normal operation of power grids [2]. The large-scale integration of renewable energy sources (RES) such as wind and solar photovoltaic generation are environmentally imperative, yet inevitably introduces unpredictability and intermittency, which are intrinsic to RES [3]. Further uncertainties may arise from the dynamic energy consumption of the industrial and residential sectors as well as electricity trading [4–6].

Understanding how the various fluctuations shape the collective dynamics of power grids is crucial for maintaining their safe operation, and has been drawing much attention over the past decade [7–19]. For instance, escape rates of the grid systems from its normal operation state have been investigated under the presence of white Gaussian noise [15], Poissonian noise [16], and Lorentzian noise [17]. Realistic fluctuations from the renewables, which are characterized by a power-law power spectral density (PSD) with Kolmogorov exponent 5/3 [3,20–22], are reported to be responsible for a higher probability of severe outages and the worsening of frequency and voltage quality [18], and found to cause a decaying variance of frequency increments over the distance and a persistant kurtosis [19].

While existing research has laid a solid foundation by examining the effects of individual or multiple noise types in isolation, these studies often restrict their focus to specific stochastic models. For instance, prior works have successfully characterized network vulnerability and escape dynamics under Gaussian white noise [15], or investigated the impact of heavy-tailed, non-Gaussian fluctuations [16]. Other studies have captured the turbulent, intermittent nature of renewable energy feed-in to assess grid stability [18] and the spatial propagation of such disturbances [19]. When colored noise models are explicitly employed, they frequently focus on specific forms with a finite correlation time, such as Ornstein-Uhlenbeck noise, to predict stochastic escape times [17] or evaluate linear transient performance metrics [10]. Despite these valuable insights into distinct noise regimes, a systematic investigation into how the continuous spectrum of general $1/f^b$ noise, spanning from white to pink and brown noise, impacts large-scale power grid dynamics remains missing up to date. Practically, $1/f^b$ noise covers diverse noise types

*Contact author: xiaozhu_zhang@tongji.edu.cn

Published by the American Physical Society under the terms of the Creative Commons Attribution 4.0 International license. Further distribution of this work must maintain attribution to the author(s) and the published article's title, journal citation, and DOI.

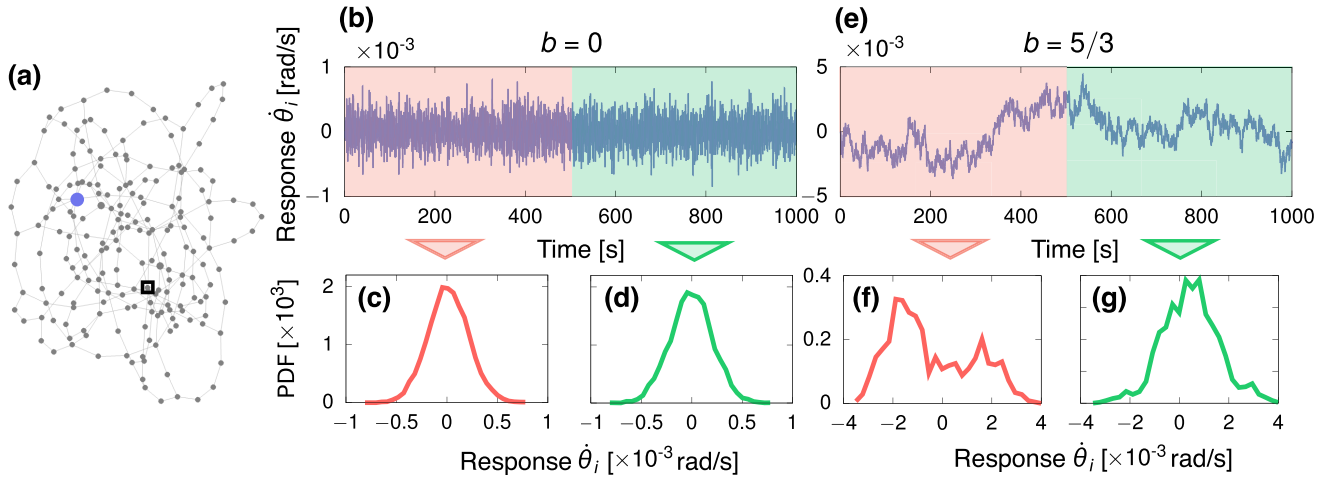


FIG. 1. Color-dependent stochastic responses induced by $1/f^b$ noise. In a random power grid network (a) generated according to Ref. [23], the stochastic responses at a single node (marked purple) induced by $1/f^b$ noise at another node (marked with a black square) are shown in (b) and (e). (b) Induced by a white noise with $b = 0$, the nodal response generates stable and Gaussian-like probability distribution functions (PDFs) (c),(d), independent of the time window of observation. PDFs (c) and (d) are generated from observation windows shaded red and green in (b). When induced by noise with a Kolmogorov exponent $b = 5/3$, characterizing the intrinsic fluctuations in the power generation from wind and solar energy [21], the nodal responses (e) generate dramatically different PDFs (f),(g) in different time windows.

pervading power grid systems, ranging from thermal white noise with $b = 0$ to electronics-based pink noise with $b = 1$ and renewable power feed-in with Kolmogorov exponent $b = 5/3$. A systematic study may help fill the gaps and establish an overarching understanding of the impact of $1/f^b$ noise on the frequency fluctuation of power systems.

In this article we systematically study how power grid networks stochastically respond to $1/f^b$ noise. By tuning the exponent b of the noise, we vary the color, i.e., the relative frequency contribution of the noise, and examine the statistical features of the grid frequency responses at distributed units in the network. We demonstrate that the grid frequency responses are stationary and Gaussian in response to $1/f^b$ noise with a flatter PSD with $b \lesssim 1$, independent of the probability distribution of the noise. We further clarify that the dominance of the low-frequency contents when $b \gtrsim 1$ may be a source of nonstationarity and non-Gaussianity of the grid frequency fluctuations and demonstrate that these results are topologically robust.

II. MODEL

A. The power grid dynamics

We adopt a paradigmatic model of power grid dyanmics [24–26] where an ac power grid system is represented as a network of N synchronous machines, each governed by second-order Kuramoto-type dynamics

$$\frac{d^2\theta_i}{dt^2} = P_i - \alpha\frac{d\theta_i}{dt} + \sum_j K_{ij}\sin(\theta_j - \theta_i) + D_i(t). \quad (1)$$

Here P_i denotes the mechanical input ($P_i > 0$) or output ($P_i < 0$) of unit i, $\alpha > 0$ the damping coefficient, and $K_{ij} = K_{ji} \geqslant 0$ the capacity of power transmission between unit j and i. θ_i represents the phase angle of synchronous machine i relative to a rotating reference frame with a nominal grid frequency, e.g., $2\pi \times 50$ Hz in Europe and many other parts of the world. In the normal operation state of power grids, i.e., without the presence of noise, the units are phaseblocked, running with a fixed state of phases. The time-dependent term $D_i(t)$ represents the external noise driving the dynamics of unit i. In this work we observe the responses in the distributed grid frequencies $\dot{\theta}_i(t)$, as it is the central observable in the monitoring, operation, and control of power grid systems [25] and exhibits intriguing statistical features in real-world data [4,27].

B. Modeling perturbed dynamics

Exposed to external disturbances, e.g., thermal white noise or the fluctuations with a Kolmogorov spectrum in the power feed-in from renewables, the entire power grid network exhibits responses with nontrivial statistical features even when the noise is only present locally, i.e., $D_i(t) \sim \delta_{ik}$ is nonzero only at a single unit k [28–32] [Fig. 1(a)]. Intriguingly, the probability distribution function (PDF) of the network response time series appear to be color dependent: they are steady and Gaussian-like, independent of the observation window if induced by white noise with $b = 0$ [see Figs. 1(b)–1(d)], but its stationarity and Gaussianity appears to be lost if induced by renewable fluctuations with $b = 5/3$ [see Figs. 1(e)–1(g)].

Therefore, in this work we focus on the impact of $1/f^b$ noise perturbing a single unit in the system by observing the stationarity and the Gaussianity of the distributed nodal responses it induces. We generate the noise by first generating white noise consisting of independent random numbers uniformly distributed in $[-1, 1]$ with a vanishing mean $\mu = 0$. Colored $1/f^b$ noise with $b \neq 0$ is then obtained by modifying the magnitude of the noise's frequency components. We multiply each component with a frequency-dependent factor proportional to $f^{-b/2}$. In this way, the $1/f^b$ noise to be implemented in the dynamical model of power grids has a definite power-law PSD with a tunable $b \in [0, 2]$ [Fig. 2(a)], but an indefinite PDF [Fig. 2(b)].

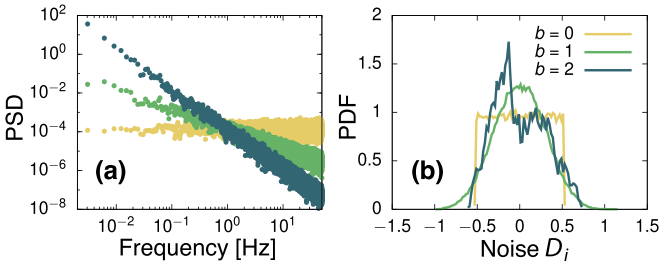


FIG. 2. The $1/f^b$ noise implemented in power grids. The power spectral density (a) and the probability distribution function (b) of three representative realizations of $1/f^b$ noise with $b = 0, 1, 2$.

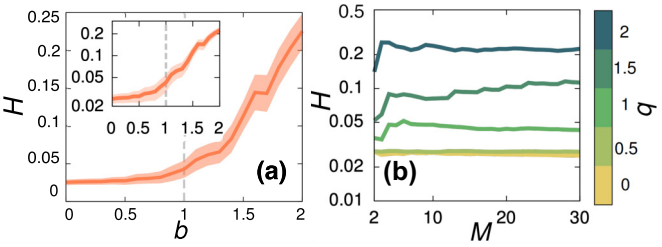


FIG. 3. The color-dependent stationarity of power grid responses. (a) The average Hellinger distance between each pair of the response PDFs obtained from 30 realizations of $1/f^b$ noise. The orange curve represents the average over all 200 nodes in the network and the shaded area indicates the standard deviation. A semilogarithmic plot is shown in the subplot. (b) Independent of the color of the noise, the Hellinger distance between PDFs across realizations remains almost the same as the number of realizations grows. The shown curves are averages over all nodes in the network. The curves are color-coded according to the noise PSD exponent b. In simulations the system parameters are set as $P_i = 1\ \mathrm{s}^{-2}$ for generators, $P_i = -1\ \mathrm{s}^{-2}$ for consumers, $K_{ij} = K = 30\ \mathrm{s}^{-2}$ for all transmission lines, and $\alpha = 1\ \mathrm{s}^{-1}$.

To better quantitatively compare the impact of noise with various color b, we fix the mean of the noise time series $\mu = 0$ and normalize the noise so that they share the same total power, which equals to its variance based on Parseval's theorem. Additionally, we rescale the noise time series so that its standard deviation $\sigma = 0.3P_i$. In our network settings, this ratio ensures that the noise is not strong enough to desynchronize the grid model system.

We examine the impact of $1/f^b$ noise on grid frequency mainly in a random power grid network [Fig. 1(a)] with its network topology generated according to Ref. [23]. We also report the robustness of the results by providing numerical evidences for another random power grid network topology generated via the same model [23], as well as for networks with diverse interaction topologies such as a chain network and a Barabási-Albert scale-free network. In the simulations we adopt the Runge-Kutta 4 integration scheme to numerically solve the network dynamics with total simulation time $T = 1000$ s and time step $\Delta t = 0.01$ s.

III. RESULTS

We perturb the 200-node random power grid model [see Fig. 1(a) for its network topology] operating at a steady state with $1/f^b$ noise impinging on a random site [marked with a black square in Fig. 1(a)] and monitor the resulting grid frequency fluctuation $\dot{\theta}_i(t)$ at each unit i (which we refer to as *responses* hereafter for brevity). Prior to any perturbations the grid is operated at a stable state where half of its nodes are randomly selected as generators with $P_i = 1\ \mathrm{s}^{-2}$ and the other half as consumers with $P_i = -1\ \mathrm{s}^{-2}$. The capacity of all transmission lines is set sufficiently large as $K_{ij} = 30\ \mathrm{s}^{-2}$, ensuring the existence of a normal operation state of the system.

Before activating noise, the network is initialized at its stable synchronous operational state, i.e., a stable fixed point obtained by solving the static nonlinear power flow equations $K_{ij} = 30\ \mathrm{s}^{-2}$ for the given network topology and power injections ($\ddot{\theta}_i = 0$, $\dot{\theta}_i = 0$ for $i = 1, \ldots, N$). The system's relaxation is governed by the slowest decaying mode of the system: With the damping coefficient $\alpha = 1\ \mathrm{s}^{-1}$, the minimum nonzero Laplacian eigenvalue $\lambda_{\min} \approx 0.247$ yields a characteristic relaxation time constant of $\tau \approx 2.25$ s [28]. Defining the transient phase as the duration required for the initial response to decay to 1/1000 of their original amplitude, its duration is estimated as $T_{\mathrm{transient}} \approx 15.6$ s. To ensure that our analysis is not corrupted by the initial transient response, we systematically discard the initial transient period of $T_{\mathrm{transient}} = 20$ s. Subsequently, the empirical probability density functions (PDFs) are constructed using the remaining post-transient data, with the number of bins fixed at $m = 35$ for all histograms.

A. Stationarity of network responses

The stationarity of a stochastic process makes it statistically tractable and allows for reliable modeling, inference, and forecasting. For the noise time series, a larger PSD exponent b implies a long-range dependence, a slow autocorrelation decay, and sometimes the nonstationarity of the noise time series. How does the nonstationarity of, e.g., the Brownian noise translate to the responses of a power grid network?

We quantify the stationarity of a nodal response by computing the Hellinger distance

$$H(P, P') := \frac{\Delta x}{\sqrt{2}} \sqrt{\sum_{i=1}^{m} (\sqrt{p_i} - \sqrt{p'_i})^2} \tag{2}$$

between the pair of response PDFs (P, P') at one specific node for different realizations of noise. Here $P = (p_1, \ldots, p_m) \in \mathbb{R}^m$ and $P' = (p'_1, \ldots, p'_m) \in \mathbb{R}^m$ represent the PDF of the nodal response with m bins and bin width Δx for two independent realizations of noise. Note that due to probability normalization, $H(P, P')$ is intrinsically bounded between 0 and 1 and remains independent of the bin number m, making additional normalization scaling unnecessary. For stationary responses, the average Hellinger distance, which is defined as a nested average computed first over all $\binom{M}{2}$ unique pairs of M independent noise realizations for each node, and subsequently averaged over all N nodes in the network, should approach zero, provided the observation window is sufficiently wide. An increase in the network-averaged Hellinger distance indicates a divergence between these PDF pairs, signifying the emergence of nonstationarity. Figure 3 shows

the average response stationarity calculated over all $N = 200$ nodes in the network using $M = 30$ noise realizations for various b. By averaging over $\binom{30}{2} = 435$ distinct pairs of these independent stochastic realizations, our evaluation strictly compares separate simulations rather than temporally correlated segments from a single history. This statistical setup ensures that the slow autocorrelation decay at large b values does not introduce evaluation artifacts, confirming H as a robust and reliable metric for capturing nonstationary transitions.

The color dependence of the response stationarity is clear. When perturbed by noise with a flatter PSD, i.e., $0 < b \lesssim 1$, the grid system yields stationary nodal responses with very low average Hellinger distances below 10^{-3} [see Fig. 3(a)]. The stationarity is consistent over all nodes in the network, as indicated by the small standard deviation of H over nodes [shaded area in Fig. 3(a)]. As the impinging noise is increasingly dominated by low-frequency components, i.e., $b \gtrsim 1$, the nodal response time series tend to be nonstationary, which is indicated by the drastically increasing average Hellinger distance [Fig. 3(a)]. Interestingly, as b exceeds 1, the level of stationarity of nodal responses disperses among individual nodes in the network, indicated by the increasing standard deviation of the nodal Hellinger distance across the network [shaded area in Fig. 3(a)]. Specifically, a semilogarithmic plot [subplot in Fig. 3(a)] reveals that the response distribution stays stationary for $b \lesssim 1$, but undergoes a sharp loss of stationarity: The average Hellinger distance exhibits an exponential-like growth once the threshold $b \approx 1$ is crossed. Moreover, we find that the stationarity of network responses persists across realizations and appears to be independent of the size of the sample sets M from which we compute the average Hellinger distance. The average distance H across realizations remains almost at the same level when the size of the sample sets M increases from around 5 [see Fig. 3(b)].

B. Gaussianity of network responses

Abundant evidence points to non-Gaussian, heavy-tailed grid frequency distributions [4,27], implying an increased risk of extreme events in power grids. Models and theories have been proposed to elucidate the relation between the probability distribution of the noise and that of the grid frequency, yet most of them are based on the Gaussianity of the noise [4], which is of limited validity in reality. Here we systematically examine the Gaussianity of the grid responses to $1/f^b$ noise with a wide range of colors.

We measure the Gaussianity of the responses using the integrated squared error (ISE) of the response PDF with respect to an analytical Gaussian distribution:

$$\mathrm{ISE}(P, G) := \frac{\Delta x}{m} \sum_{i=1}^{m} (p_i - g_i)^2. \tag{3}$$

Here $P = (p_1, \ldots, p_m) \in \mathbb{R}^m$ is the empirical response PDF, Δx denotes the bin width, m denotes the number of bins, and $G = (g_1, \ldots, g_m) \in \mathbb{R}^m$ is the corresponding analytical Gaussian fit. The ISE quantifies the global discrepancy between the empirical response distribution and its analytical Gaussian fit, serving as a sensitive metric to capture its deviations from

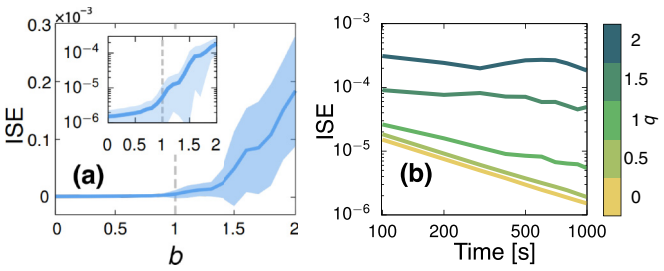


FIG. 4. The color-dependent Gaussianity of the response PDFs. (a) The mean square error χ^2 of fitting the response PDF to a Gaussian distribution, averaged over all nodes and over 30 realizations, increases drastically as b exceeds a point around 1. The shaded area indicates the standard deviation of the data set. A semilogarithmic plot is shown in the subplot. (b) The Gaussianity of the PDF for $b \lesssim 1$ is established as the fit error χ^2 decreases as a power law with an increasing observation time, while the error stays at a high level for $b \gtrsim 1$. The curves in (b) are color-coded according to the color of the noise b. In simulations we use the same system parameters as for Fig. 3.

Gaussianity. Consequently, the overall (non-)Gaussianity of the network responses is represented by the average ISE computed across all nodes in the network. We test the Gaussianity of the grid responses for 30 realizations of $1/f^b$ noise for various b, and the average response (non-)Gaussianity is shown in Fig. 4. The Gaussianity of the responses once more exhibits an evident dependence on the noise color (Fig. 4). For noise with a flatter power spectrum ($0 < b \lesssim 1$), the responses at all nodes appear to be consistently Gaussian, indicated by a close-to-zero average fit error and a very low standard deviation among nodes and realizations [see Fig. 4(a)]. Interestingly, this result holds even though the noise impinging on the system is non-Gaussian [Fig. 2(b)]. As the exponent b exceeds a point around 1 and the low-frequency components gain more weight in the driving signal, the response's non-Gaussianity increases drastically, which is reflected in the exponentially growing average fit error for $b \gtrsim 1$ [Fig. 4(a)]. For $b \lesssim 1$, the response's Gaussianity, as a theoretical limit at $t \to \infty$, is further corroborated by the power-law decay of the fit error with an extending observation time [Fig. 4(b)]. In contrast, for $b \gtrsim 1$, the fit error stays at a high level, indicating zero tendency of the responses towards Gaussianity.

The transition near $b \approx 1$ can be understood from the competition between the noise correlation time τ_c and the system relaxation time τ_{relax}. For $1/f^b$ noise, τ_c is finite for $b < 1$ and diverges as b approaches and exceeds 1 [33]. When $\tau_c \ll \tau_{\mathrm{relax}}$ ($b \lesssim 1$), the noise decorrelates much faster than the system relaxes, producing many independent perturbations. The cumulative response is then stationary and, by the central limit theorem, Gaussian. When $\tau_c \gg \tau_{\mathrm{relax}}$ ($b \gtrsim 1$), τ_c diverges. The noise maintains its direction over times comparable to or longer than τ_{relax}, continuously driving the system away from the fixed point. The central limit theorem no longer applies, and the response becomes nonstationary and non-Gaussian. From the perspetive of time series analysis, for $b \gtrsim 1$, the noise PSD is heavily dominated by the low-frequency components, which induce a slow, long-term drift in the grid's response within the observation window. When aggregating

response data over this window, the slow drift manifests as heavy-tailed, non-Gaussian distributions due to the shifting mean of the local fluctuations.

C. Topological robustness

The color dependence of the Gaussianity and the stationarity of grid responses appear to be robust against the change of the interaction topology of the underlying network. In this section we present numerical results demonstrating the validity of the results we have shown in Secs. III A and III B for networks with diverse topologies.

We observe the grid responses in three networks: a chain network, another random power grid network (different from the one shown in Fig. 1), and a Barabási-Albert scale-free network [topologies shown in the insets of Figs. 5(a)–5(c)]. We obtain almost identical color dependences of the stationarity and Gaussianity of grid responses (Fig. 5). For all three tested network topologies, the average run-to-run PDF difference measured by the Hellinger distance H and the fit error of the nodal response PDFs to Gaussian distributions both show drastic surges as the color exponent of the noise b exceeds a critical value around 1, indicating the loss of stationarity and Gaussianity for $b \gtrsim 1$.

Additionally, to ensure the universality and robustness of our findings, we systematically evaluate the transition behavior under various parameter regimes (e.g., different damping coefficient, heterogeneity levels of coupling strengths, distribution of power generators, and network sizes). The onset of nonstationarity and non-Gaussianity remains qualitatively robust across all tested configurations (see the Supplemental Material [34] for the complete set of robustness results).

IV. CONCLUSION

To sum up, in this work we identify a direct, causal link between the color of $1/f^b$ noise and the emergence of anomalous statistical states in power grid frequency. Specifically, we provide a systematic numerical investigation suggesting the loss of stationarity and Gaussianity in the frequency responses as the noise's PSD exponent b, characterizing the color of the noise, exceeds a critical value around 1. The stationarity and the Gaussianity of the resposnes for $b \lesssim 1$ appears to be independent of the probability distribution of the noise. These conclusions are validated by abundant numerical simulations and are shown to be independent of the specific configuration of the network interaction structure. The observed transition near $b \approx 1$ coincides with the onset of divergence of the noise correlation time at $b = 1$ and the resulting breakdown of the central limit theorem, which occurs when the effective number of independent perturbations becomes too small.

These findings thereby constitute a foundational step towards a more comprehensive understanding of the collective responses of power grids operating under colored noise from technical and environmental sources, and as well provide practical guidelines in grid operation and control. One of the consequential implications of our finding is that, the present Kolmogorov fluctuations in the renewable power feed-in in modern power grids have a characteristic PSD exponent

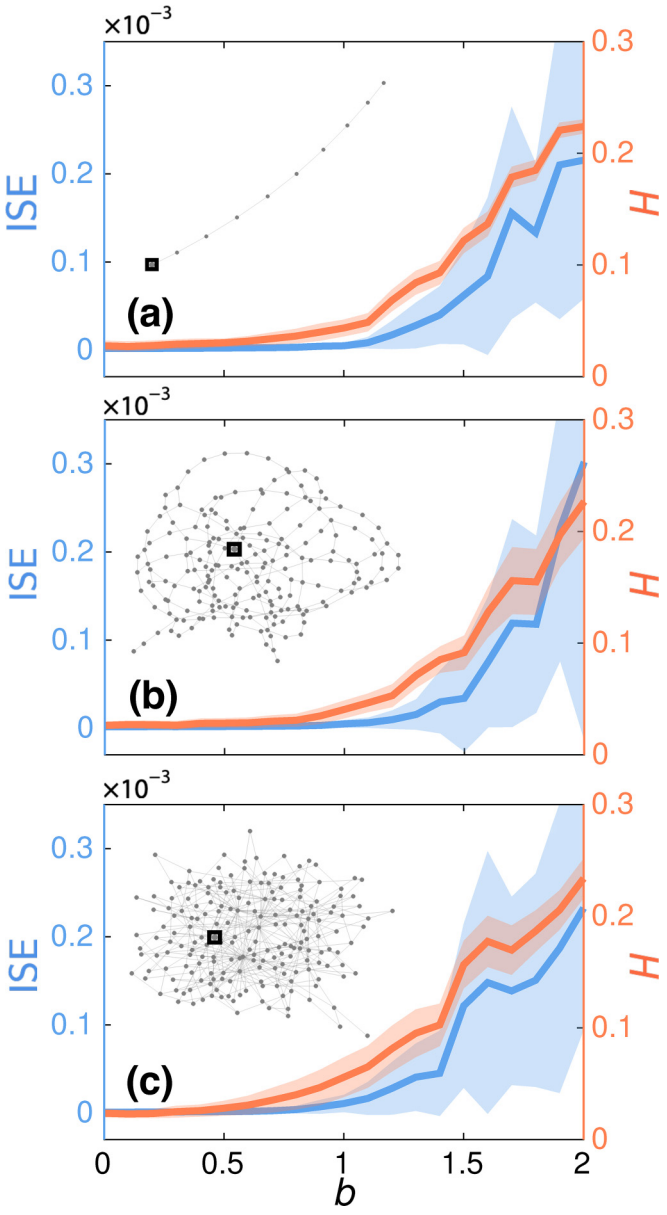


FIG. 5. Robust transition of stationarity and Gaussianity across interaction topologies. The loss of Gaussianity and stationarity of responses at $b \approx 1$ appears to be robust for (a) a chain network, (b) a random power grid network generated via [23], and (c) a Barabási-Albert scale-free network. The average fit error χ^2 to a Gaussian distribution and the average Hellinger distance H between nodal response PDFs across 30 realizations, are shown with blue and orange curves, respectively. The standard deviation of the data set is indicated by the shaded area around the curve. The site of the noise is marked with a black square in the respective sketch of networks [insets of (a), (b), and (c)]. In simulations we use the same system parameters as for Fig. 3 except $N = 10, 200, 200$ for (a)–(c).

5/3 falling in the interval $b \gtrsim 1$, and thus would induce *nonstationary* and *non-Gaussian* responses in power grid frequency. Such responses are statistically distinctive to the Gaussian responses induced by, e.g., thermal noise with a broad flat power spectrum, and may be one of the sources of the non-Gaussianity in the frequency distribution observed in real-world datasets [4,27]. Comparing our simulation

results with empirical measurements, we find qualitative consistency with the heavy-tailed frequency distributions documented in power grids. This agreement suggests that the colored-noise-driven dynamics captured in our numerical simulations are not merely theoretical constructs but bear tangible relevance to real-world grid behavior. In practice, the nonstationary and non-Gaussian responses are intrinsically hard to predict and risky, requiring varied control strategies and contingency plans.

Future research on noise-induced network responses might include quantitative predictions of the statistical characteristics and even go beyond the overall statistical properties and investigate intriguing transient response behaviors; for instance, the spikes induced by sudden changes in the impinging noise time series, e.g., the intermittencies that frequently occur in renewable power sources such as wind and solar voltaic generation. These spikes usually have node-specific magnitudes that bring nontrivial risks to the safe operation of real-world networked systems.

ACKNOWLEDGMENTS

We thank Prof. Marc Timme for insightful discussions and valuable suggestions. This project is funded by the National Natural Science Foundation of China (Grants No. 12375036 and No. 12350710786).

DATA AVAILABILITY

The data that support the findings of this article are openly available [35].

[1] E. Marris, Energy: Upgrading the grid, Nature (London) **454**, 570 (2008).
[2] J. A. Turner, A realizable renewable energy future, Science **285**, 687 (1999).
[3] P. Milan, M. Wächter, and J. Peinke, Turbulent character of wind energy, Phys. Rev. Lett. **110**, 138701 (2013).
[4] B. Schäfer, C. Beck, K. Aihara, D. Witthaut, and M. Timme, Non-Gaussian power grid frequency fluctuations characterized by Lévy-stable laws and superstatistics, Nat. Energy **3**, 119 (2018).
[5] M. Anvari, L. R. Gorjão, M. Timme, D. Witthaut, B. Schäfer, and H. Kantz, Stochastic properties of the frequency dynamics in real and synthetic power grids, Phys. Rev. Res. **2**, 013339 (2020).
[6] M. Anvari, E. Proedrou, B. Schäfer, C. Beck, H. Kantz, and M. Timme, Data-driven load profiles and the dynamics of residential electricity consumption, Nat. Commun. **13**, 4593 (2022).
[7] D. Witthaut, F. Hellmann, J. Kurths, S. Kettemann, H. Meyer-Ortmanns, and M. Timme, Collective nonlinear dynamics and self-organization in decentralized power grids, Rev. Mod. Phys. **94**, 015005 (2022).
[8] B. Li and K. Y. Michael Wong, Optimizing synchronization stability of the Kuramoto model in complex networks and power grids, Phys. Rev. E **95**, 012207 (2017).
[9] L. Tumash, S. Olmi, and E. Schöll, Effect of disorder and noise in shaping the dynamics of power grids, Europhys. Lett. **123**, 20001 (2018).
[10] T. Coletta, B. Bamieh, and P. Jacquod, Transient performance of electric power networks under colored noise, in *2018 Proceedings of IEEE Conference on Decision and Control (CDC)* (IEEE, Miami Beach, FL, 2018), pp. 6163–6167.
[11] S. Auer, F. Hellmann, M. Krause, and J. Kurths, Stability of synchrony against local intermittent fluctuations in tree-like power grids, Chaos **27**, 127003 (2017).
[12] J. C. Lacerda, J. Dias, C. Freitas, and E. Macau, Vulnerability and stability of power grids modeled by second-order Kuramoto model: A mini review, Eur. Phys. J.: Spec. Top. **230**, 3509 (2021).
[13] T. Ritmeester and H. Meyer-Ortmanns, Rare desynchronization events in power grids: On data implementation and dimensional reductions, J. Phys.: Complexity **3**, 045010 (2022).
[14] X. Qing, W. He, M. Zhou, and W. Du, Quantifying fluctuations for dynamical power systems with stochastic excitations: A power spectral density-based method, Chaos **33**, 053113 (2023).
[15] B. Schäfer, M. Matthiae, X. Zhang, M. Rohden, M. Timme, and D. Witthaut, Escape routes, weak links, and desynchronization in fluctuation-driven networks, Phys. Rev. E **95**, 060203(R) (2017).
[16] J. Hindes, P. Jacquod, and I. B. Schwartz, Network desynchronization by non-Gaussian fluctuations, Phys. Rev. E **100**, 052314 (2019).
[17] M. Tyloo, R. Delabays, and P. Jacquod, Noise-induced desynchronization and stochastic escape from equilibrium in complex networks, Phys. Rev. E **99**, 062213 (2019).
[18] K. Schmietendorf, J. Peinke, and O. Kamps, The impact of turbulent renewable energy production on power grid stability and quality, Eur. Phys. J. B **90**, 222 (2017).
[19] H. Haehne, K. Schmietendorf, S. Tamrakar, J. Peinke, and S. Kettemann, Propagation of wind-power-induced fluctuations in power grids, Phys. Rev. E **99**, 050301 (2019).
[20] J. Apt, The spectrum of power from wind turbines, J. Power Sources **169**, 369 (2007).
[21] M. Anvari, G. Lohmann, M. Wächter, P. Milan, E. Lorenz, D. Heinemann, M. R. R. Tabar, and J. Peinke, Short term fluctuations of wind and solar power systems, New J. Phys. **18**, 063027 (2016).
[22] M. Anvari, B. Werther, G. Lohmann, M. Wächter, J. Peinke, and H.-P. Beck, Suppressing power output fluctuations of photovoltaic power plants, Solar Energy **157**, 735 (2017).
[23] P. Schultz, J. Heitzig, and J. Kurths, A random growth model for power grids and other spatially embedded infrastructure networks, Eur. Phys. J.: Spec. Top. **223**, 2593 (2014).
[24] G. Filatrella, A. H. Nielsen, and N. F. Pedersen, Analysis of a power grid using a Kuramoto-like model, Eur. Phys. J. B **61**, 485 (2008).
[25] J. Machowski, J. Bialek, and J. Bumby, *Power System Dynamics: Stability and Control* (Wiley, New York, 2011).
[26] A. E. Motter, S. A. Myers, M. Anghel, and T. Nishikawa, Spontaneous synchrony in power-grid networks, Nat. Phys. **9**, 191 (2013) .

[27] L. Rydin Gorjão, R. Jumar, H. Maass, V. Hagenmeyer, G. Cigdem Yalcin, J. Kruse, M. Timme, C. Beck, D. Witthaut, and B. Schäfer, Open database analysis of scaling and spatio-temporal properties of power grid frequencies, Nat. Commun. **11**, 6362 (2020).

[28] X. Zhang, S. Hallerberg, M. Matthiae, D. Witthaut, and M. Timme, Fluctuation-induced distributed resonances in oscillatory networks, Sci. Adv. **5**, eaav1027 (2019).

[29] S. Kettemann, Delocalization of disturbances and the stability of ac electricity grids, Phys. Rev. E **94**, 062311 (2016).

[30] S. Tamrakar, M. Conrath, and S. Kettemann, Propagation of disturbances in AC electricity grids, Sci. Rep. **8**, 6459 (2018).

[31] X. Zhang, C. Ma, and M. Timme, Vulnerability in dynamically driven oscillatory networks and power grids, Chaos **30**, 063111 (2020).

[32] X. Zhang, D. Witthaut, and M. Timme, Topological determinants of perturbation spreading in networks, Phys. Rev. Lett. **125**, 218301 (2020).

[33] M. Keshner, 1/f noise, Proc. IEEE **70**, 212 (1982).

[34] See Supplemental Material at http://link.aps.org/supplemental/10.1103/tr4w-yrs1 for detailed results on the parameter robustness of the stationarity and Gaussianity transition.

[35] L. Yang and X. Zhang, https://github.com/longit-git/power_grid_noise_color.git.